Micron 160 (2022) 103327

Contents lists available at ScienceDirect

Micron

journal homepage: www.elsevier.com/locate/micron

Micro-computed tomography for analysis of heavy metal accumulation in the opercula

Dominik Panek [a,*], Bartosz Leszczyński [a,*], Dorota Wojtysiak [b], Ewa Drąg-Kozak [c], Ewa Stępień [a]

[a] Department of Medical Physics, M. Smoluchowski Institute of Physics, Faculty of Physics, Astronomy and Applied Computer Science, Jagiellonian University, ul. Łojasiewicza 11, 30-348 Kraków, Poland
[b] Department of Genetics, Animal Breeding and Ethology, University of Agriculture in Krakow, al. Mickiewicza 24/28, 30-059 Krakow, Poland
[c] Department of Animal Nutrition and Biotechnology, and Fisheries, University of Agriculture in Krakow, al. Adama Mickiewicza 24/28, 30-059 Kraków, Poland

ARTICLE INFO

Keywords:
Micro-CT
Micro-computed tomography
Operculum
Heavy metals
Accumulation
Fish

ABSTRACT

Micro-computed tomography (micro-CT) provides numerous opportunities in biomedical research. It allows the examination of samples in a non-destructive manner and visualization of the inner structures of various biological and nonbiological objects. This study was conducted to evaluate the potential of micro-CT scanner in the assessment of heavy metal accumulation in the opercula. The samples were taken from Prussian carp (*Carassius gibelio*) exposed to waterborne Cd (4.0 mg/L), Zn (4.0 mg/L), and the mixture of these two metals (4.0 mg Cd/L and 4.0 mg Zn/L) for 28 days. Heavy metal concentrations were determined using atomic absorption spectrometry. The results demonstrated higher concentrations of Cd and Zn in the treatment group opercula samples compared with the control group opercula samples. A simple micro-CT scan was performed to verify whether heavy metal accumulation could be determined in the reconstructed images. The results showed that micro-CT is potentially a powerful tool for metal accumulation detection. Moreover, it allowed visualization of the examined samples, revealing regions of heavy metal accumulation and providing the opportunity to compare samples exposed to different types of heavy metals.

1. Introduction

Micro-computed tomography (micro-CT; μCT) enables the imaging of various types of organic and inorganic structures in a non-destructive manner with a high spatial resolution, usually less than 5 μm (du Plessis and Broeckhoven, 2019; Ehling, 2014; Salmon and Sasov, 2007; Stauber and Müller, 2008). Initially, micro-CT was predominantly used in the field of material sciences, where it was a powerful tool for examining diverse materials, especially to analyze their porosity (Baptista, 2021; Jiang, 2017; Zhao, 2016). Recently, micro-CT has become a popular imaging modality in biological research. Primarily, micro-CT was used to visualize mineralized tissues or parts of the tissues, with densities significantly different from their surroundings (Zhao, 2016; Tang, 2013; Leszczyński et al., 2014; Tomaszewska et al., 2018). Furthermore, micro-CT can be used for molecular imaging, including imaging of three-dimensional cell structures such as spheroids, owing to its high spatial resolution (Ito, 2005; Wyss, 2009; Karimi et al., 2020). The biomedical application of micro-CT is increasing and new application areas are being found. The use of staining combined with micro-CT enables the analysis and visualization of soft tissue, such as tumors or vasculature (Tielemans et al., 2020; Leszczyński et al., 2018; Kirschner, 2015).

In aquatic environments, the sources of heavy metals are natural and anthropogenic. The degree of metal accumulation in fish tissues depends on the type of contamination, metal type, fish species, fish size, age, geographical distribution, trophic level, and feeding behavior.

This study considered heavy metal accumulation in the opercula, which is a novel approach, while several studies have considered heavy metal accumulation in fish soft tissues, such as muscles or inner organs. The significance of this research is associated with the hazardous impact on the health of humans with the consumption of fish exposed to heavy metals, which has been widely reported in several studies (Bawuro et al., 2018; Shafiuddin Ahmed, 2019). However, heavy metal accumulation is not limited to fishes. In some studies, bioaccumulation of Cd in chicken embryos has been studied, and many adverse effects have been reported (Krzysztof et al., 2013). Nevertheless, there is little research considering the use of micro-CT to evaluate heavy metal accumulation, and the available studies have focused mostly on plants. Kaiser et al. (Kaiser,

* Corresponding authors.
E-mail addresses: dominik.panek@doctoral.uj.edu.pl (D. Panek), bartosz.leszczynski@uj.edu.pl (B. Leszczyński).

https://doi.org/10.1016/j.micron.2022.103327
Received 15 February 2022; Received in revised form 7 July 2022; Accepted 7 July 2022
Available online 10 July 2022

2005) showed that micro-CT can be a useful supplementary technique to assess the accumulation of different heavy metals, such as Cu and Pb, emphasizing the use of micro-CT to visualize the root fragments of white rocket *Diplotaxis erucoides*. The plants were grown in the presence of a solution with high concentrations of Cu or Pb, which accumulated in specific cells in the root and was evident from the visualizations. Metscher et al. (Metscher, 2009) considered the accumulation of heavy metals in the case of specimen staining, enabling the distinction of soft tissues with similar X-ray attenuation coefficients. The lack of intensive research in this field provides a great opportunity for new uses of micro-CT in biomedical research.

Additionally, analysis of the X-ray attenuation distribution provides both qualitative and quantitative information regarding the distribution of heavy metals in the sample (Byers et al., 2019). Therefore, micro-CT can be a useful tool in analyzing heavy metal accumulation or can be advantageous as a complementary non-destructive tool for techniques such as X-ray fluorescence (XRF), which may require powdered samples, as shown in (Byers et al., 2019).

This study aimed to evaluate the potential of micro-CT examination to detect heavy metal accumulation in the opercula. The main goals were to determine the occurrence and regions of accumulation.

2. Materials and methods

2.1. Samples

The experimental treatments were conducted on Prussian carp (*Carassius gibelio*) females at the age of 3 years obtained from the ponds of the Experimental Station of the Department of Animal Nutrition and Biotechnology, and Fisheries of the University of Agriculture in Krakow, Poland.

Fish were exposed to a sublethal concentration of 4.0 mg/L Zn, 4.0 mg/L Cd, or 4.0 mg/L Zn + 4.0 mg/L Cd for 28 days. Zn and Cd concentrations were chosen considering the levels of these metals present in surface waters, ranging from 1 to > 16 mg/L (Obasi and Akudinobi, 2020; Witeska et al., 2010; da Silva, 2017). After exposure, the operculum from the fish in each group was used to determine the Cd and Zn concentrations. The experiment was approved by the Local Animal Ethics Committee of Krakow, Poland (approval no. 144/2019).

2.2. Atomic absorption spectrometry

The preparation of tissue (operculum) for heavy metal analysis and determination of the metal concentration were conducted as per a previous study (Drąg-Kozak, 2018). Metal levels in the opercula were analyzed by atomic absorption spectrometry (AAS) using a Model ATI UNICAM 929 (Unicam Ltd., Cambridge, UK). The results were expressed as mg (of Cd and Zn) per kg of wet tissue weight (w.w.). Differences in the concentrations of Zn and Cd between the control and treatment samples were calculated using Student's t-test. The normality of the data distribution was tested using the Shapiro-Wilk test, and the homogeneity of variance was tested using the Levene test.

2.3. Micro-CT protocol and imaging

In this study, a microCT scanner (Bruker SkyScan 1172) with an 8 W X-ray tube was used. The scanning parameters were as follows: voltage, 80 kV; amperage, 100 μA; rotation step, 0.3°; detector resolution, 2000 × 666 px; pixel size, 5 μm; and an aluminum filter (thickness, 0.5 mm). The experimental workflow was identical for all examined samples. The only exception was the scanning time, which ranged from 2 to 4 h depending on the size of the sample. Samples that underwent a scan were placed in a specially designed 3D printed holder presented in Fig. 1. The holder was adapted to fit the three opercula simultaneously. Two millimeter Styrofoam discs were used as specimen spacers.

In this study, six samples were designated as the control group (not exposed to heavy metals) and 14 as the treatment group (five were exposed to Zn, three to Cd, and six to a combination of Zn and Cd).

Three different software packages were used to obtain the desired visualizations. NRecon (Skyscan, Bruker microCT, version 1.7.3.1) enabled the reconstruction of images after selecting an appropriate dynamic range. The lower boundary was set to exclude air from the images, and the upper boundary was set to the maximum registered attenuation coefficient to avoid clipping of data. This procedure provided the same grayscale for all images. CTAn (Skyscan, Bruker microCT, version 1.16.1.0) allowed for choosing an adequate region of interest (ROI) from the scanned specimens, from which the data were collected in order to create histograms of shades of gray. CTVox (Skyscan, Bruker microCT, version 3.3.0 r1403) enabled the creation of three-dimensional visualizations of the examined samples by volume rendering, which mapped different shades of gray to the colors of interest and correlated with higher or lower densities in the specific regions of the samples (Kaiser, 2005).

3. Results

3.1. Heavy metals concentration assessment

The results of the heavy metal concentration assessment in the opercula (using AAS) are presented in Tables 1 and 2. Statistically significant differences in the mean values of concentration between different groups were determined using the Student's t-test and are marked with asterisks. The concentration of heavy metals was significantly different in the treatment groups compared to the control group.

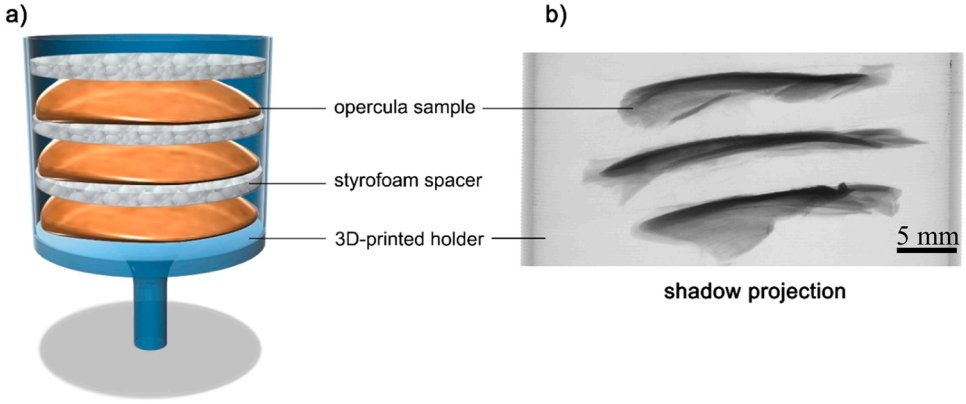

Fig. 1. Samples setup for micro-CT scan: (a) model of 3D-printed holder with 3 opercula samples (orange) and styrofoam spacers; (b) shadow projection image of opercula samples in the holder, the styrofoam spacers are transparent for 80 keV X-ray.

Table 1
Zinc wet weight (w.w.) concentrations in the fish opercula after 28 days of Zn intoxication. Range is defined as the difference between the highest and lowest measured value.

Group	Zinc mean concentration, mg/kg w.w.	Range, mg/kg w.w.	p-value
Control	114.99	10.10	–
Zinc	158.62 *	13.56	0.0002
Zinc and cadmium	137.95 *	29.90	0.0087
Cadmium	113.78 ns	8.21	0.6927

*Statistical significance compared to the control group, ns – not significant.

Table 2
Cadmium wet weight (w.w.) concentrations in the fish opercula after 28 days of Cd intoxication. The range is defined as the difference between the highest and lowest measured value.

Group	Cadmium mean concentration, mg/kg w.w.	Range, mg/kg w.w.	p-value
Control	0.06	0.02	–
Zinc	0.13 *	0.06	0.0013
Zinc and cadmium	0.39 *	0.12	< 0.0001
Cadmium	1.27 *	0.47	0.0015

*Statistical significance compared with the control group.

3.2. Micro-CT

Histograms were created for all the samples (Fig. 2) to represent the cumulative relative volume depending on the grayscale value. Evidently, the distribution of the grayscale values differed for the treatment and control samples. The distribution of grayscales shifted ("stretched") towards higher values for samples exposed to metals having higher atomic numbers, reaching ~ 190 for samples exposed to a mixture of Cd and Zn, while for the control sample, the highest grayscale value was 162.

These results suggested further quantitative investigation of the differences between all samples by subtracting the mean distributions of grayscale values of the control group samples from those of the treatment group samples. This differential analysis allowed us to obtain the information about the area under the distributions and the localization of the maximum of a given distribution (x_c). Heavy metals with higher densities had a higher x_c value, and the area under the histograms was equal to 1.79%, 5.63%, and 7.22% for Zn, Cd, and the mixture of Zn and Cd respectively – Fig. 3. Additionally, the lognormal curves were fitted to see how well they can model given data. This type of fit was chosen because the shape of the differential curves resulting from subtraction is characterized by significant skewness.

All fitted curves were characterized by high goodness-of-fit parameters (R^2), with values of 0.97, 0.98, and 0.99 for the upper – a), middle – b), and lower – c) graphs, respectively (Fig. 3). Graphs with fitted curves can be found in the supplementary materials. Visualization of the examined samples was also performed (Fig. 4). The areas of heavy metal accumulation are shown in blue.

4. Discussion

In the quantitative analysis of heavy metal accumulation, AAS confirmed that the levels of heavy metal accumulation were significantly higher in the treated groups than in the control (Tables 1 and 2). The significance of these results was confirmed using Student's t-test, with a significance level of 0.05. However, the levels of zinc in the examined samples were relatively high, even in the control group, because fish bones constitute the main and highly preserved reservoir of minerals, especially Ca, Zn, P, and Mn (Witeska et al., 2010; Baeverfjord, 2019). The results derived from micro-CT indicated that the grayscale histograms shifted towards higher values, which was presumably the result of heavy metal accumulation (Fig. 2). A higher density in a given region corresponded to a higher attenuation coefficient, and thus the absorption of radiation in this area increased. The tendency to reach higher grayscale values with increasing metal density was true for all the examined samples. Thus, the order of increasing maximal grayscale value was: control sample (162) < zinc-exposed sample (175) < cadmium-exposed sample (187) < zinc- and cadmium-exposed sample (190). These results are consistent with theoretical predictions because the linear absorption coefficient was higher at higher densities. Heavy metals with higher densities had a higher x_c value, which in turn corresponded to a higher grayscale value. Furthermore, the area under the histograms provided additional information regarding heavy metal accumulation. This area corresponded to the volume of tissue exposed to heavy metals. Thus, the samples with the mixture of Cd and Zn indicated that these two heavy metals did not exhibit combined accumulation, as they were found to accumulate separately because the area under the curve for the Zn and Cd samples (Fig. 3) was approximately equal to the sum of Cd and Zn (7.22%). In addition, lognormal curves fitted to the

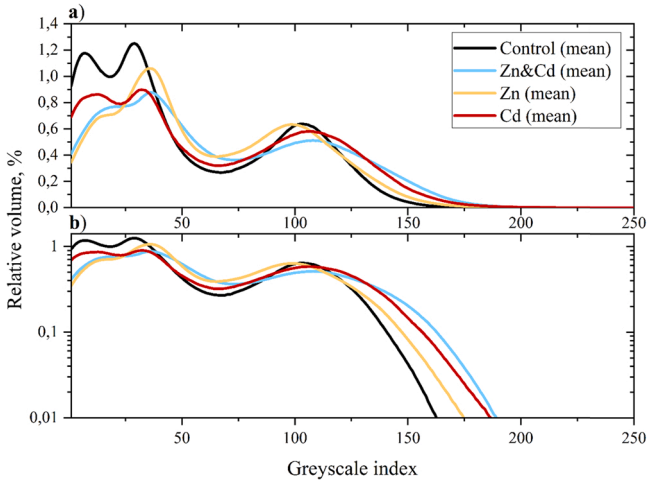

Fig. 2. Comparative distributions showing the greyscale values for all the examined samples. The a) plot is the simple distribution of greyscale values, and b) is its logarithmic version.

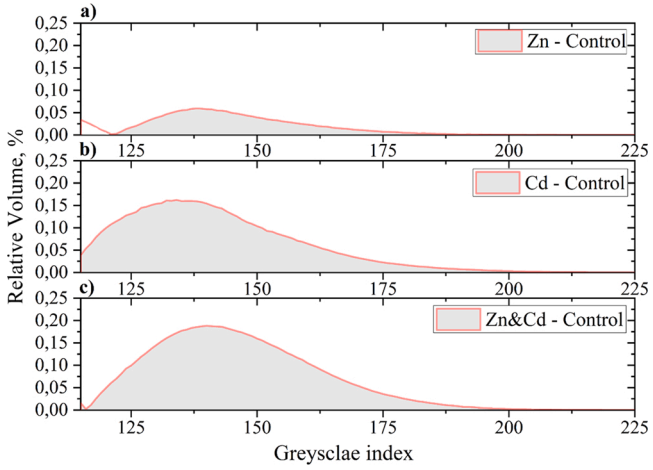

Fig. 3. Differential analysis. The red curves represent the empirical data, after subtracting the heavy metal distributions from the control distributions. Grey color represents the area under given distribution. Plot a) represents subtracted Zn and control distribution, b) represents subtracted Cd and control distribution, c) represents subtracted Zn and Cd mixture and control distribution.

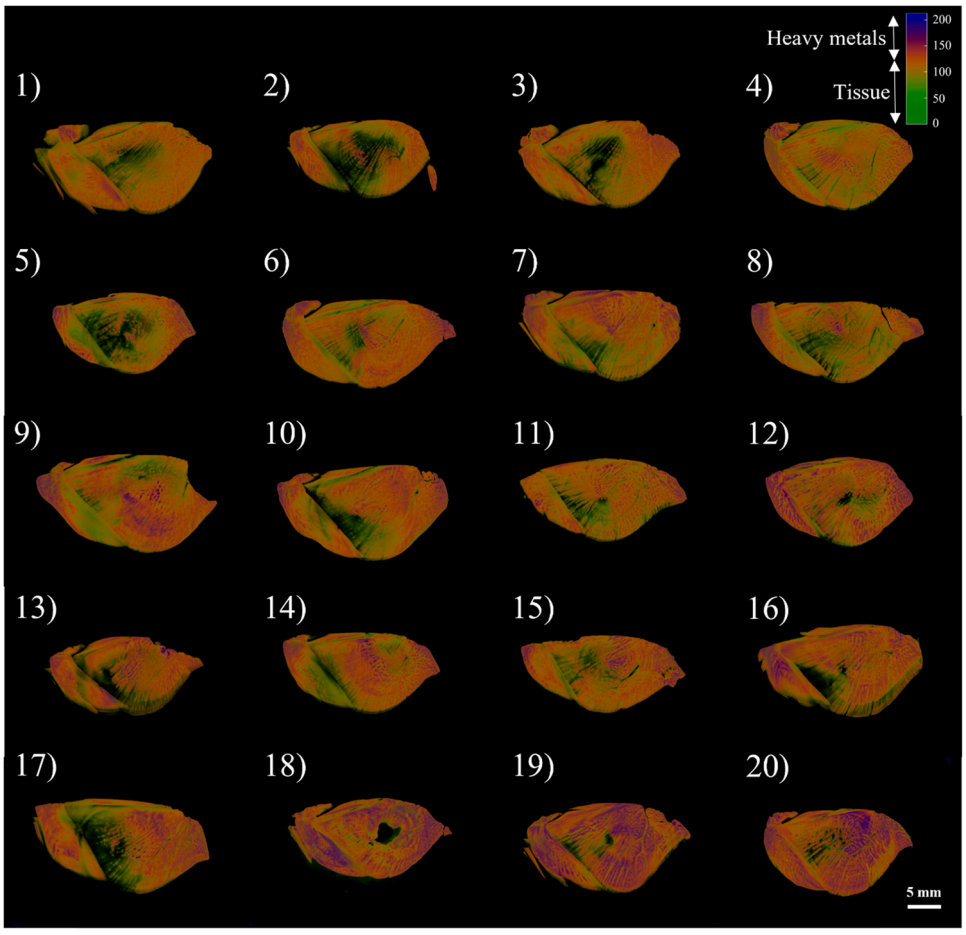

Fig. 4. Visualizations showing the distribution of the accumulation of heavy metals. The blue and purple areas of the figure correspond to the higher opacity and can be interpreted as the accumulation of heavy metals in a given region. Numbers 1–6 describe the control group, numbers 7–11 describe the opercula exposed to Zn, numbers 12–14 describe the opercula exposed to Cd, and numbers 15–20 describe the opercula exposed to the mixture of Zn and Cd.

data with high R^2 parameter ($\geq$0.97) proved that this type of distribution may be used in the future to obtain additional information about the heavy metal accumulation. Moreover, our results are consistent with those obtained using the AAS technique, which also confirms that micro-CT is a unique and advantageous tool for detection of heavy metal accumulation. 3D visualizations show clearly the areas of heavy metal accumulation. The intensities of these areas differed significantly between the control and treatment groups. The densest area is visible in opercula 15–20, which referred to the Zn- and Cd-exposed samples (Fig. 4). This visualization facilitated identification of the main regions of accumulation and their intensity.

5. Conclusions

The ability to predict heavy metal accumulation without destroying the examined sample is a notable achievement. Micro-CT provided consistent results in comparison to AAS with respect to heavy metal accumulation assessment. 3D visualization clearly indicates of the regions of their increased uptake. Further research focusing on soft tissues could also be helpful, as fish are a very common food source worldwide. Our research proves that a noninvasive method for examining samples (using micro-CT) and estimating the regions of heavy metal accumulation should be taken into consideration in future research.

In conclusion, micro-CT is a remarkable tool in this field of study, not only as a supplementary technique, but also on its own. In the case of quantitative analysis (AAS), the results demonstrated that the concentrations of Cd and Zn accumulated in the opercula increased in comparison to the levels of these metals in the control fish, which proves that exposure led to the uptake of the above-mentioned metals in the opercula.

Declaration of Competing Interest

The authors declare that they have no known competing financial interests or personal relationships that could have appeared to influence the work reported in this paper.

Data Availability

Data will be made available on request.

Acknowledgements

This research was supported by the subvention of the Department of Animal Nutrition and Biotechnology, and Fisheries no. 020011-D015, Poland.

References

Baeverfjord, G., 2019. Mineral nutrition and bone health in salmonids. Rev. Aquac. 11, 740–765.

Baptista, R., 2021. Experimental and numerical characterization of 3D-printed scaffolds under monotonic compression with the aid of micro-CT volume reconstruction. Bio-Des. Manuf. 4, 222–242.

Bawuro, A.A., Voegborlo, R.B., Adimado, A.A., 2018. Bioaccumulation of heavy metals in some tissues of fish in lake Geriyo, Adamawa State, Nigeria. J. Environ. Public Health 2018.

Byers, H.L., McHenr, L.J., Grundl, T.J., 2019. XRF techniques to quantify heavy metals in vegetables at low detection limits. Food Chem.: X 1.
da Silva, Y., 2017. Bedload as an indicator of heavy metal contamination in a Brazilian anthropized watershed. Catena 153, 106–113.
Drąg-Kozak, E., 2018. Protective effect of melatonin on cadmium-induced changes in some maturation and reproductive parameters of female Prussian carp (Carassius gibelio B.). Environ. Sci. Pollut. Res. 25, 9915–9927.
Ehling, J., et al., 2014. Micro-CT imaging of tumor angiogenesis: quantitative measures describing micromorphology and vascularization. Am. J. Pathol. 184, 431–441.
Ito, M., 2005. Assessment of bone quality using micro-computed tomography (micro-CT) and synchrotron micro-CT. J. Bone Miner. Metab. 23, 115–121.
Jiang, L., 2017. Permeability estimation of porous media by using an improved capillary bundle model based on micro-CT derived pore geometries. Heat. Mass Transf. /Waerme- und Stoff. 53, 49–58.
Kaiser, J., 2005. Mapping of the metal intake in plants by large-field X-ray microradiography and preliminary feasibility studies in microtomography. Eur. Phys. J. D. 32, 113–118.
Karimi, H., Leszczyński, B., Kołodziej, T., Kubicz, E., Przybyło, M., Stępień, E., 2020. X-ray microtomography as a new approach for imaging and analysis of tumor spheroids. Micron 137.
Kirschner, S., 2015. In vivo micro-CT imaging of untreated and irradiated orthotopic glioblastoma xenografts in mice: capabilities, limitations and a comparison with bioluminescence imaging. J. Neuro-Oncol. 122, 245–254.
Krzysztof, P., Małgorzta, D., Dorota, W., Marcin, L., Jerzy, N., 2013. Effect of in ovo injection of cadmium on chicken embryo heart. Afr. J. Agric. Res. 8, 1534–1539.
Leszczyński, B., Skrzat, J., Kozerska, M., Wróbel, A., Walocha, J., 2014. Three dimensional visualisation and morphometry of bone samples studied in microcomputed tomography (micro-CT). Folia Morphol. 73, 422–428.
Leszczyński, B., Sojka-Leszczyńska, P., Wojtysiak, D., Wróbel, A., Pędrys, R., 2018. Visualization of porcine eye anatomy by X-ray microtomography. Exp. Eye Res. 167, 51–55.
Metscher, B.D., 2009. Micro CT for comparative morphology: Simple staining methods allow high-contrast 3D imaging of diverse non-mineralized animal tissues. BMC Physiol. 9.
Obasi, P.N., Akudinobi, B.B., 2020. Potential health risk and levels of heavy metals in water resources of lead–zinc mining communities of Abakaliki, southeast Nigeria. Appl. Water Sci. 10.
du Plessis, A., Broeckhoven, C., 2019. Looking deep into nature: a review of micro-computed tomography in biomimicry. Acta Biomater. 85, 27–40.
Salmon, P.L., Sasov, A.Y., 2007. Advanced Bioimaging Technologies in Assessment of the Quality of Bone and Scaffold Materials: Techniques and Applications. Springer Berlin Heidelberg, pp. 323–331.
Shafiuddin Ahmed, A.S., 2019. Bioaccumulation of heavy metals in some commercially important fishes from a tropical river estuary suggests higher potential health risk in children than adults. PLoS One 14.
Stauber, M., Müller, R., 2008. Micro-computed tomography: A method for the non-destructive evaluation of the three-dimensional structure of biological specimens. Methods Mol. Biol. 455, 273–292.
Tang, R., et al., 2013. Micro-computed tomography (Micro-CT): A novel approach for intraoperative breast cancer specimen imaging. Breast Cancer Res. Treat. 139, 311–316.
Tielemans, B., Dekoster, K., Verleden, S.E., Sawall, S., Leszczyński, B., Laperre, K., et al., 2020. From mouse to man and back: closing the correlation gap between imaging and histopathology for lung diseases. Diagnostics 10 (9), 636.
Tomaszewska, I.M., Leszczyński, B., Wróbel, A., Gładysz, T., Duncan, H.F., 2018. A micro-computed tomographic (micro-CT) analysis of the root canal morphology of maxillary third molar teeth. Ann. Anat. 215, 83–92.
Witeska, M., Bilska, K., Sarnowski, P., 2010. Effects of copper and cadmium on growth and yolk utilization in Barbel (Barbus barbus L.) Larvae. Pol. J. Environ. Stud. 19, 227–230.
Wyss, C., 2009. Molecular imaging by micro-CT: specific E-selectin imaging. Eur. Radiol. 19, 2487–2494.
Zhao, Y., et al., 2016. Visualization of asphaltene deposition effects on porosity and permeability during CO_2 flooding in porous media. J. Vis. 19, 603–614.